An Autoinhibitory Peptide from the Erythrocyte Ca-ATPase Aggregates and Inhibits Both Muscle Ca-ATPase Isoforms

Laxma G. Reddy,* Yongli Shi,* Howard Kutchai,§ Adelaida G. Filoteo,# John T. Penniston,# and David D. Thomas*

*Department of Biochemistry, University of Minnesota Medical School, Minneapolis, Minnesota 55455; #Department of Biochemistry and Molecular Biology, Mayo Clinic, Rochester, Minnesota 55902; and §Department of Molecular Physiology and Biological Physics, University of Virginia, Charlottesville, Virginia 22908 USA

ABSTRACT We have studied the effects of C28R2, a basic peptide derived from the autoinhibitory domain of the plasma membrane Ca-ATPase, on enzyme activity, oligomeric state, and E1-E2 conformational equilibrium of the Ca-ATPase from skeletal and cardiac sarcoplasmic reticulum (SR). Time-resolved phosphorescence anisotropy (TPA) was used to determine changes in the distribution of Ca-ATPase among its different oligomeric species in SR. C28R2, at a concentration of 1–10 μM, inhibits the Ca-ATPase activity of both skeletal and cardiac SR (CSR). In skeletal SR, this inhibition by C28R2 is much greater at low (0.15 μM) than at high (10 μM) Ca^{2+}, whereas in CSR the inhibition is the same at low and high Ca^{2+}. The effects of the peptide on the rotational mobility of the Ca-ATPase correlated well with function, indicating that C28R2-induced protein aggregation and Ca-ATPase inhibition are much more Ca-dependent in skeletal than in CSR. In CSR at low Ca^{2+}, phospholamban (PLB) antibody (functionally equivalent to PLB phosphorylation) increased the inhibitory effect of C28R2 slightly. Fluorescence of fluorescein 5-isothiocyanate-labeled SR suggests that C28R2 stabilizes the E1 conformation of the Ca-ATPase in skeletal SR, whereas in CSR it stabilizes E2. After the addition of PLB antibody, C28R2 still stabilizes the E2 conformational state of CSR. Therefore, we conclude that C28R2 affects Ca-ATPase activity, conformation, and self-association differently in cardiac and skeletal SR and that PLB is probably not responsible for the differences.

INTRODUCTION

The SERCA-type Ca-ATPases pump Ca^{2+} from sarcoplasm into the sarcoplasmic reticulum (SR) lumen to allow relaxation of muscle. The plasma membrane Ca-ATPase (PMCA)-type Ca-ATPase pumps Ca^{2+} into the cell across the plasma membrane. Although the sequence homology is only 30% between SERCA1-type pumps (usually obtained from rabbit fast-twitch muscle) and PMCA-type pumps (usually obtained from human erythrocytes), secondary structure predictions suggest similarities in the overall arrangement of important structural and functional domains (Verma et al., 1988; Strehler, 1991). Cardiac SR (CSR) Ca-ATPase (SERCA2a, usually obtained from dog hearts) is regulated by phospholamban (PLB) (Lindemann et al., 1983), which inhibits the cardiac Ca-ATPase by decreasing its apparent affinity for Ca^{2+}. This inhibition, which is observed only at submicromolar Ca^{2+}, is released upon phosphorylation of PLB either by cAMP-dependent protein kinase (PKA) or by Ca-calmodulin-dependent protein kinase II (CaM kinase II). The PMCA-type Ca-ATPases are regulated directly by the binding of calmodulin to a highly basic C-terminal region (autoinhibitory domain) of PMCA, stimulating the pump by increasing both Ca^{2+} affinity (a decrease in K_M) and maximum velocity (V_{max}) (Enyedi and Penniston, 1993). Photoactivable derivatives of PLB and the calmodulin-binding domain of PMCA, respectively, have been shown to cross-link to their respective pumps at structurally homologous regions (Enyedi and Penniston, 1993). Although the regulatory mechanisms of SERCA and PMCA by phospholamban and calmodulin, respectively, are well established at the functional level, the physical mechanism of interaction of these regulatory molecules with the pumps and the resulting physical changes in the pumps are not understood at the molecular level.

Previous investigations into the regulatory mechanisms of the SR Ca-ATPase in skeletal muscle have established the importance of the oligomeric state of the Ca-ATPase to its enzymatic function (Squier et al., 1988a; Voss et al., 1991; Karon and Thomas, 1993). Agents that aggregate the Ca-ATPase in skeletal SR, such as chemical cross-linkers, the amphipathic peptide melittin, or the local anesthetic lidocaine, inhibit enzymatic activity (Squier et al., 1988a; Mahaney and Thomas, 1991; Voss et al., 1991; Kutchai et al., 1994). Agents that dissociate aggregates of the Ca-ATPase, such as the volatile anesthetics ether and halothane, activate the enzyme (Bigelow and Thomas, 1987; Birmachu et al., 1989; Karon and Thomas, 1993).

In CSR, PLB inhibits the enzymatic activity of the Ca-ATPase (James et al., 1989a; Sham et al., 1991) at low Ca^{2+} (submicromolar) concentrations, and this inhibition correlates with a decreased rotational mobility of the Ca-ATPase, compared to the rotational mobility at high Ca^{2+} or after PLB phosphorylation (Voss et al., 1994). Upon PLB phosphorylation or addition of micromolar Ca^{2+} (high Ca^{2+}), the resting inhibition of the Ca-ATPase is relieved (the

Received for publication 13 July 1998 and in final form 15 March 1999.

Address reprint requests to Dr. David D. Thomas, Department of Biochemistry, University of Minnesota Medical School, 4-225 Millard Hall, 435 Delaware St. SE, Minneapolis, MN 55455. Tel.: 612-625-0957; Fax: 612-624-0632; E-mail: ddt@ddt.biochem.umn.edu.

0006-3495/99/06/3058/08 $2.00

enzyme is activated), and this activation correlates with an increase in the rotational mobility of the Ca-ATPase. Thus the regulation of CSR Ca-ATPase by phosphorylation and dephosphorylation of PLB may involve the self-association and dissociation of the Ca-ATPase.

C28R2, an amphipathic peptide, corresponds to 28 residues of the highly basic C-terminal calmodulin-binding domain of the erythrocyte plasma membrane Ca-ATPase (rPMCA2b). This region of the PMCA forms part of the enzyme's autoinhibitory domain, which shares functional features with PLB (Vorherr et al., 1992). It has been reported that this positively charged peptide inhibits both PMCA and the skeletal SR Ca-ATPase (Enyedi and Penniston, 1993). The aim of the present study is to characterize the effects of C28R2 on the enzymatic activity and oligomeric state of the Ca-ATPase in both cardiac and skeletal SR. Because the rotational dynamics and oligomeric state of the Ca-ATPase play key roles in modulating Ca-ATPase activity, it is important to understand the underlying mechanisms relating these physical properties to the enzyme's kinetic behavior. The results shed light on similarities and differences in the physical principles that govern the enzymatic mechanisms and regulation of these three different Ca-ATPase systems.

MATERIALS AND METHODS

Reagents

Erythrosin-5-isothiocyanate (ErITC) and fluorescein-5-isothiocyanate (FITC) were obtained from Molecular Probes (Eugene, OR) and stored in *N,N′*-dimethylformamide (DMF) under liquid nitrogen. Catalase, glucose oxidase, β-D-glucose, pyruvate kinase, lactate dehydrogenase, phosphoenol pyruvate, ATP, and NADH (β-nicotinamide adenine dinucleotide, reduced form) were purchased from Sigma (St. Louis, MO). The calcium ionophore A23187 was obtained from Calbiochem (San Diego, CA). C28R2 peptide was synthesized chemically (Enyedi et al., 1991) and dissolved in water containing 1 mM dithiothreitol (DTT). The monoclonal anti-PLB antibody 2D12 (PLB Ab) (Cantilina et al., 1993) was kindly provided by Dr. Larry Jones (University of Indiana).

Preparation of SR

All SR preparations were made at 4°C. SR vesicles were prepared from the fast twitch skeletal muscle of New Zealand white rabbits (Fernandez et al., 1980), then purified on a discontinuous sucrose gradient (Birmachu et al., 1989) to separate Ca-ATPase-rich light SR (LSR) from heavy and intermediate SR vesicles (junctional SR-containing calcium release proteins). LSR was resuspended in 0.3 M sucrose, 20 mM 3-(*N*-morpholino)propanesulfonic acid (MOPS) (pH 7.0); rapidly frozen in 4-mg aliquots; and stored in liquid nitrogen until use. Based on sodium dodecyl sulfate-polyacrylamide gel electrophoresis, LSR contained ~7 nmol Ca-ATPase/mg SR protein, corresponding to 80% of the total protein by weight. The LSR vesicles thus prepared are tightly sealed, as indicated by Ca^{2+} ionophore (A23187) stimulation of ATPase activity. Cardiac sarcoplasmic reticulum (CSR) prepared from canine ventricular tissue was kindly provided by Dr. Joseph J. Feher (Feher and Briggs, 1983).

ATPase assay

Ca-ATPase activity was measured at 25°C using an enzyme-linked, continuous spectrophotometric assay (Karon et al., 1994). The standard assay mix contained between 5 and 50 μg of SR vesicles in 0.5 ml of buffer containing 50 mM MOPS (pH 7.0), 60 mM KCl, 2 mM $MgCl_2$, 5 mM EGTA, 0.42 mM phosphoenolpyruvate, 0.15 mM NADH, 3.75 I.U. of pyruvate kinase, and 9.0 I.U. of lactate dehydrogenase. The assay mixture also contained 1 μg/ml of the ionophore A23187 (added from DMF; the final DMF concentration was less than 1%, v/v) to prevent a buildup of calcium inside the vesicles that might inhibit the Ca-ATPase activity. An aliquot of $CaCl_2$ solution was added to the assay mix to give either 10 μM (high Ca^{2+}) or 0.15 μM (low Ca^{2+}) free Ca^{2+}. C28R2 dissolved at 1.0 mg/ml in water containing 1 mM DTT was added to the samples and allowed to incubate for 5 min before data collection. Mg-ATP (to a final concentration of 1 mM) was added to start the assay, and the absorbance of NADH was followed at 340 nm to determine the amount of ATP hydrolyzed. Experiments in the presence of PLB Ab were performed by incubating Ab (1:2 Ab:Ca-ATPase by weight) at 25°C for 20 min before the start of the ATPase assay.

Labeling of LSR with ErITC and FITC

For phosphorescence experiments, the Ca-ATPase in SR vesicles was specifically labeled with ErITC as described previously (Birmachu and Thomas, 1990), and the final labeled LSR was suspended in 25 mM MOPS (pH 7.0), 0.3 M sucrose, and 0.1 mM $CaCl_2$. For fluorescence experiments, the Ca-ATPase in SR was specifically labeled with FITC as described previously (Voss et al., 1995).

Fluorescence of FITC-labeled SR

The fluorescence intensity of 1 μM FITC-SR was measured with a SPEX Fluorolog II fluorimeter (λ_{ex} = 495 nm, λ_{em} = 520 nm) by summing the total fluorescence emission over 20 s. This was repeated four times per sample. The experiments were performed in the standard buffer containing 50 mM MOPS, 60 mM KCl, 2 mM $MgCl_2$, and 1 mM EGTA, or 0.1 mM $CaCl_2$ (pH 7.0). Fluorescence changes were calculated as described previously, after the addition of $CaCl_2$ or EGTA (Karon et al., 1994).

Time-resolved phosphorescence anisotropy

Phosphorescence anisotropy was measured in a buffer containing 50 mM MOPS (pH 7.0), 60 mM KCl, 2 mM $MgCl_2$, 5 mM EGTA, with $CaCl_2$ added to give the required free [Ca^{2+}]. Oxygen was enzymatically removed from the sample by the addition of 200 μg/ml glucose oxidase, 30 μg/ml catalase, and 5 mg/ml β-D-glucose (Eads et al., 1984). Deoxygenation was carried out in a sealed cuvette containing 0.2–0.3 mg of SR protein/ml for 15–25 min before phosphorescence data collection. C28R2 stock solution was added to the SR in a manner analogous to that used for ATPase activity measurements. Phosphorescence anisotropy decays were obtained as described previously (Ludescher and Thomas, 1988). The time-dependent anisotropy $r(t)$ is given by

$$r(t) = (I_{vv} - GI_{vh})/(I_{vv} + 2GI_{vh}) \quad (1)$$

where I_{vv} and I_{vh} are obtained by signal-averaging the time-dependent phosphorescence decays following 2000 laser pulses, with a single detector and a polarizer that alternates between the vertical (I_{vv}) and horizontal (I_{vh}) positions every 2000 pulses. The laser repetition rate was 200 Hz, so a typical $r(t)$ acquisition required 4 min to complete 10 loops, or cycles of 4000 laser pulses each (2000 in each orientation). G is an instrumental correction factor, determined by measuring the anisotropy of free dye in solution under experimental conditions.

TPA data analysis

Phosphorescence anisotropy decays were analyzed as described previously (Birmachu and Thomas, 1990), using a nonlinear least-squares fit to a sum

of exponentials plus a constant:

$$r(t)/r(0) = \sum_{i=1}^{3} A_i e^{-t/\Phi_i} + A_\infty \quad (2)$$

where ϕ_i are rotational correlation times, A_i are normalized amplitudes (r_i/r_o), A_∞ is the normalized final anisotropy (r_∞/r_o), and r_o is the initial anisotropy ($r(0) = r_0 = \Sigma r_i + r_\infty$). The goodness of fit for the anisotropy decays was evaluated by comparing χ^2 values for the multiexponential fits and by comparing plots of the residuals (the difference between the measured and the calculated decays). Phosphorescence lifetimes were determined by fitting the total intensity ($I_{vv} + 2I_{vh}$) to a sum of exponentials in a manner analogous to that of the anisotropy decay fitting (Birmachu and Thomas, 1990). C28R2, at the concentrations used in the experiments, did not have significant effects on phosphorescence lifetimes.

In the present study we have also fit data to an analytical uniaxial rotation model (Belford et al., 1972) that explicitly incorporates all of the factors that determine the anisotropy decay kinetics of uniaxially rotating chromophores:

$$r(t) = \sum_{i=1}^{n} x_i r_i(t) + x_1 r_0 \quad (3)$$

where x_i is the mole fraction associated with the ith rotating species, and x_1 is the mole fraction of Ca-ATPase that does not rotate on the time scale of the experiment (immobile Ca-ATPase). Using this expression, changes in the mole fraction of immobile Ca-ATPase induced by SR perturbants can be directly determined, independently of the orientation of the probe (Mersol et al., 1995).

The expression for the individual anisotropy of the ith uniaxially rotating species (Szabo, 1984) is

$$r_i(t) = \kappa(a_1 e^{-D_i t} + a_2 e^{-4D_i t} + a_3) \quad (4)$$

where

$$a_1 = 1.2(\sin\theta_a \cos\theta_a \sin\theta_e \cos\theta_e \cos\Phi_{ae}) \quad (5a)$$

$$a_2 = 0.3(\sin^2\theta_a \sin^2\theta_e \cos 2\Phi_{ae}) \quad (5b)$$

$$a_3 = 0.2(3\cos^2\theta_a - 1)(3\cos^2\theta_e - 1) \quad (5c)$$

Here D_i is the rotational diffusion coefficient about an axis normal to the plane of the membrane, θ_a and θ_e are the angles between the probe's absorption and emission dipoles and the membrane normal, ϕ_{ae} is the azimuthal angle between the absorption and emission transition dipoles of the probe, and κ is the order parameter for fast (submicrosecond) rotation of the probe with respect to the protein. The submicrosecond motion may result from the site of probe attachment undergoing segmental motion or from partial freedom of motion of the probe itself around its site of attachment.

The uniaxial rotation model (Eqs. 3–5) explicitly accounts for 1) the biexponential decay for each species (Eq. 4), 2) the order parameter κ for submicrosecond motion, and 3) the angular dependence of the amplitudes of the exponentially decaying terms (Eqs. 5a–5c). We have observed previously that transient phosphorescence anisotropy decays of ErITC-labeled skeletal and CSR are best fit by including three uniaxially rotating species (Karon et al., 1995; Mersol et al., 1995). Each species is assumed to have the same values of θ_a, θ_e, and ϕ_{ae}, and to differ from the other species only in its diffusion coefficient, presumably because of differences in aggregation state. Thus the n-component uniaxial model (Eqs. 4 and 5) has three more variables to be fit than the n-component exponential model (Eq. 3), but the addition of each component adds just two new parameters for each model.

RESULTS

Effects of C28R2 on Ca-ATPase activity in LSR and CSR

Enyedi and Penniston (1993) reported that C28R2 inhibited Ca-ATPase activity in skeletal SR. We have measured the effects of C28R2 on Ca-ATPase activity in skeletal and CSR at low (150 nM) and high (10 μM) Ca^{2+}. Our results show that this peptide at micromolar concentration strongly inhibits Ca-ATPase activity not only in skeletal SR, but also in CSR, and that the inhibition occurs at both high and low Ca^{2+} concentrations (Fig. 1). In skeletal SR, inhibition was substantially greater at low Ca^{2+} than at high Ca^{2+} (Fig. 1 *A*), whereas in CSR, the inhibition was essentially independent of [Ca^{2+}] (Fig. 1 *B*). At low Ca^{2+}, the inhibition by C28R2 is greater in skeletal SR than in CSR; at high Ca^{2+}, inhibition was greater in CSR than in skeletal SR. In skeletal SR, C28R2 was shown to be very effective in increasing the $K_{0.5}$ for Ca^{2+} and decreasing the maximum velocity of the enzyme (Enyedi and Penniston, 1993). In CSR, our studies indicate that C28R2 effects only the maximum velocity of the enzyme (Fig. 2).

To determine whether the differences between skeletal and CSR are due to the presence of phospholamban (PLB) in CSR, we tested the effects of C28R2 on CSR in the presence of PLB Ab, which is functionally equivalent to PLB phosphorylation, relieving the inhibition that is caused by PLB at low Ca^{2+} (Cantilina et al., 1993). PLB Ab had no significant effect on the C28R2-induced inhibition of Ca-ATPase in CSR at low Ca^{2+} (Fig. 3). We also measured the effects of C28R2 on Ca-ATPase activity in CSR after removing PLB with Triton (Nakamura et al., 1983) and did not observe a significant change in [Ca^{2+}] dependence (data not shown). It is clear that the different [Ca^{2+}] dependence of inhibition by C28R2 is due to isoform differences, not to PLB.

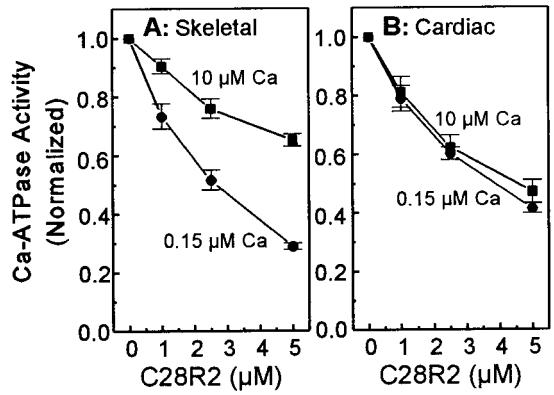

FIGURE 1 Effect of C28R2 on Ca-ATPase activity (normalized to the activity in the absence of C28R2 at each Ca^{2+} concentration), in skeletal SR (*A*) and CSR (*B*), at 10 μM Ca^{2+} (■) and 0.15 μM Ca^{2+} (●), at 25°C. Mean ± SEM (n = 3).

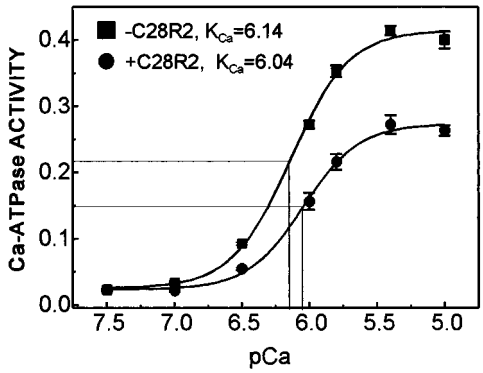

FIGURE 2 Ca^{2+} dependence of Ca-ATPase activity in CSR in the absence (■) and presence (●) of 15 μM C28R2, at 25°C. Mean ± SEM (n = 3).

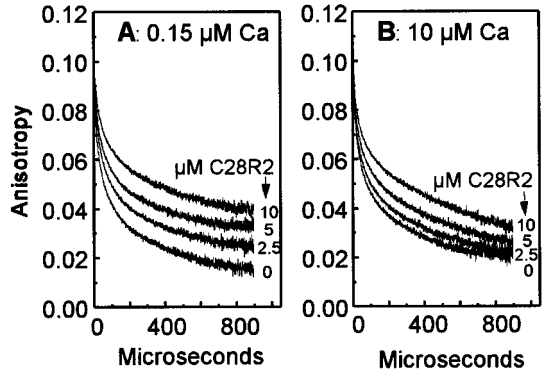

FIGURE 4 Time-resolved phosphorescence anisotropy (TPA) decays of ErITC-labeled skeletal SR at 0.15 μM Ca^{2+} (A) and 10 μM Ca^{2+} (B), in the presence of the indicated concentrations of C28R2, at 25°C.

Effects of C28R2 on the rotational dynamics of the Ca-ATPase

We used time-resolved phosphorescence anisotropy (TPA) to determine the effects of C28R2 on the rotational dynamics of the Ca-ATPase in skeletal and CSR at high and low Ca^{2+}. When C28R2 was added to ErITC-labeled skeletal SR, it decreased the amplitude of decay of anisotropy in a concentration-dependent manner (Fig. 4), resulting in an increase in the final anisotropy (A_∞). Anisotropy decay rates did not change significantly compared to the amplititudes of the decay, in response to the concentration of C28R2. Similar effects were observed in CSR at low and high Ca^{2+} (Fig. 5). The decays were best fit to a sum of three exponentials plus a constant residual anisotropy (Eq. 2, n = 3), as described previously (Birmachu and Thomas, 1990; Karon and Thomas, 1993; Mersol et al., 1995). The three components represent approximately the rotational mobility of Ca-ATPase monomers (A_1), small oligomers (A_2), and larger oligomers (A_3). The final anisotropy (A_∞) increases with the mole fraction of species that are too large to rotate appreciably on the time scale of the experiment (Eq. 3) (Birmachu and Thomas, 1990). C28R2 increased the rotational correlation times (decreased rotational rates) of all three rotating components slightly in LSR, but had little effect on the rotational correlation times in CSR. As indicated in the Discussion, similar conclusions were reached when the more explicit uniaxial diffusion model (Eqs. 4 and 5) was considered.

In skeletal SR, treatment with C28R2 increased the value of A_∞ (Fig. 6 A), with a decrease in the amplitudes associated with smaller ATPase oligomers (A_1 and A_2). Values of A_3 (larger, but not immobile, oligomers) were increased at high Ca^{2+}, but changed only slightly at low Ca^{2+}. In CSR, C28R2 also resulted in an increase in the proportion of the immobile species, A_∞ (Fig. 6 B), with decreases in the values of A_1, A_2, and A_3, suggesting that C28R2 induces the formation of large, immobile oligomers from monomers and larger mobile oligomers. In skeletal SR, increased A_∞ induced by C28R2 is more extensive at low Ca^{2+} than at high Ca^{2+} (Fig. 6 A). However, in CSR, we did not observe any significant difference in the increase in A_∞ caused by C28R2 at high and low Ca^{2+} (Fig. 6 B).

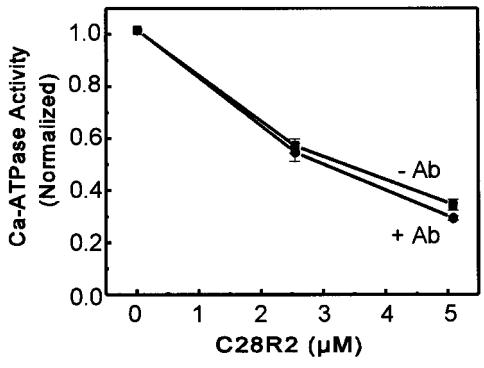

FIGURE 3 Effect of C28R2 on Ca-ATPase activity (normalized to the activity in the absence of C28R2 at each Ca^{2+} concentration) in CSR at 0.15 μM Ca^{2+} (low Ca) in the absence (■) and presence (●) of PLB Ab, at 25°C. Mean ± SEM (n = 3).

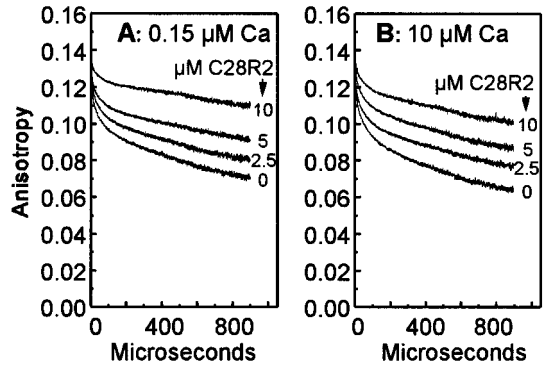

FIGURE 5 Time-resolved phosphorescence anisotropy (TPA) decays of ErITC-labeled CSR at 0.15 μM Ca^{2+} (A) and 10 μM Ca^{2+} (B), in the presence of the indicated concentrations of C28R2.

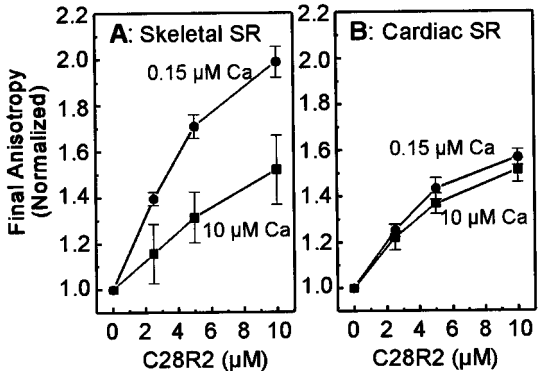

FIGURE 6 Effects of C28R2 on the final anisotropy (A_∞) of ErITC-labeled skeletal SR (*A*) and CSR (*B*) at 10 μM Ca^{2+} (■) and 0.15 μM Ca^{2+} (●). A_∞ was determined by fitting the TPA decay to Eq. 2, then normalized to the control (no C28R2). Mean ± SEM (n = 3).

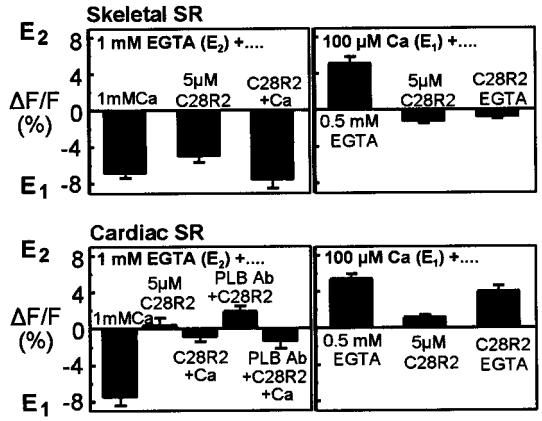

FIGURE 7 Fluorescence intensity changes of FITC-labeled SR in response to C28R2. Fluorescence intensity changes were measured in standard buffer containing either 1 mM EGTA (control, represents E2 state) or 100 μM Ca^{2+} (control, represents E1 state) at 25°C. C28R2 (5 μM) was added to FITC-labeled SR in standard buffer containing either 1 mM EGTA or 100 μM Ca^{2+} in the absence or presence of PLB Ab (for CSR in EGTA), followed by the addition of either 1 mM Ca^{2+} (to EGTA buffer to change [Ca^{2+}] from 0 to 20 μM) or 0.5 mM EGTA (to Ca^{2+} buffer to change [Ca^{2+}] from 100 μM to 100 nM). The fluorescence intensities were measured before and after the addition of either EGTA or Ca^{2+} and expressed as a percentage change. Fluorescence changes were calculated as described previously (Karon et al., 1994). Data represent the mean ± SEM (n = 3).

Effects of C28R2 on the fluorescence of FITC-labeled skeletal and CSR

The fluorescence intensity of covalently bound FITC, a fluorescent probe similar in structure to ErITC, is sensitive to the E1/E2 conformational changes in the Ca-ATPase. Although it is not possible to determine quantitatively the E1/E2 equilibrium constant from FITC fluorescence, we can determine the direction in which this equilibrium is perturbed (Froud and Lee, 1986; Sagara et al., 1992). These changes probably reflect changes in rate constants, which in turn determine enzyme turnover rates. The addition of Ca^{2+} after EGTA decreases FITC fluorescence, indicating a decrease in E2/E1 (Fig. 7, *left panels*), whereas the addition of EGTA after Ca^{2+} increases fluorescence, indicating a decrease in E2/E1 (Fig. 7, *right panels*).

In FITC-labeled skeletal SR, C28R2 decreased fluorescence, indicating a decrease in E2/E1, at both low Ca^{2+} (Fig. 7, *top left panel*) and high Ca^{2+} (Fig. 7, *top right panel*). In contrast, in FITC-labeled CSR, C28R2 increased fluorescence, indicating an increase in E2/E1, at both low Ca^{2+} (Fig. 7, *lower left panel*) and high Ca^{2+} (Fig. 7, *lower right panel*). This different response to the peptide in skeletal and CSR was not affected by PLB Ab (Fig. 7, *lower left*), indicating that PLB is not responsible for the difference.

DISCUSSION

Effects of C28R2 on Ca-ATPase activity

It has been found previously that the positively charged amphipathic peptide melittin inhibits the Ca-ATPase of skeletal SR while inducing large-scale aggregation of the enzyme through electrostatic interactions (Voss et al., 1995). Systematically decreasing the positive charge of melittin by acetylation decreased the inhibition and oligomerization of the Ca-ATPase (Voss et al., 1995). Similarly, the positively charged local anesthetic lidocaine inhibits and aggregates the Ca-ATPase in both skeletal and CSR, suggesting that lidocaine-induced inhibition may be due to cationic interaction with the hydrophilic (anionic) cytoplasmic domain of the Ca-ATPase (Karon et al., 1995). Similarly, it has been suggested that phospholamban (PLB) interacts with the cardiac Ca-ATPase, through its positively charged cytoplasmic domain, and inhibits pump activity while inducing large-scale aggregation of the pump (Voss et al., 1994, 1995). Ca-pump aggregation, like inhibition, is induced by PLB only at low Ca^{2+} and can be relieved by either PLB phosphorylation or micromolar Ca^{2+} (Voss et al., 1994). The positively charged synthetic peptide C28R2 has been shown to inhibit PMCA-type Ca-ATPase (Enyedi et al., 1991) and the SERCA1 Ca-ATPase in skeletal SR (Enyedi and Penniston, 1993). The inhibition by this peptide is due to its direct interaction with the pump, rather than to an effect on membrane permeability or on a Ca^{2+} channel (Enyedi and Penniston, 1993).

In the present study, we found that C28R2 at micromolar levels strongly inhibits Ca-ATPase activity both in skeletal and CSR (Fig. 1). In skeletal SR, we found that this inhibition is greatest at submicromolar Ca^{2+} (Fig. 1 *A*), confirming previous reports that this peptide decreases not only the maximum velocity of SERCA1 at micromolar Ca^{2+} (V_{max}), but also the apparent Ca^{2+} affinity ($K_{0.5}$) (Enyedi and Penniston, 1993). In contrast, we report that the C28R2 inhibition in CSR (SERCA2a) is Ca-independent (Fig. 1 *B*), and the effect is only on maximum velocity (V_{max}) (Fig. 2). This could be due either to a structural difference between the two isoforms, or to the presence of phospholamban (PLB) in CSR. However, the addition of PLB Ab to CSR, which eliminates the influence of PLB on the Ca-ATPase

(Cantilina et al., 1993), did not significantly change the extent of inhibition of the Ca-ATPase by C28R2 at low Ca^{2+} (0.15 μM) (Fig. 3), where the effects of PLB are greatest (Tada and Katz, 1982). We conclude that the two Ca-ATPase isoforms differ in their susceptibility to C28R2, suggesting either a difference in the binding site for this peptide, or a difference in the effect of Ca^{2+} on this site. These results also suggest that the binding site on the Ca-ATPase and the mechanism of inhibition are different for C28R2 and PLB.

The apparent K_I for inhibition of the Ca-ATPase by C28R2 is in the range of 2–5 μM. Because this is significantly higher than the concentration of the Ca-ATPase in enzymatic and spectroscopic measurements, and because peptide binding was not measured directly, we cannot rule out the possibility that the binding stoichiometry is greater than 1, i.e., that there might not be a single site on the pump for binding and inhibition. Similarly, the stoichiometry and specificity whereby phospholamban inhibits the SERCA2a pump are not known.

Effects of C28R2 on the oligomeric state of the Ca-ATPase

Previous studies of both skeletal and CSR demonstrated that several perturbants that inhibit the Ca-ATPase activity also promote the formation of larger oligomers of the pump (Bigelow et al., 1986; Bigelow and Thomas, 1987; Squier and Thomas, 1988; Squier et al., 1988a; Birmachu and Thomas, 1990; Karon and Thomas, 1993; Voss et al., 1991, 1994). In contrast, perturbants that promote the dissociation of larger oligomers of the Ca-ATPase into smaller oligomers consistently increased its activity (Voss et al., 1991, 1994; Kutchai et al., 1994; Mahaney et al., 1992). In the present study, TPA was used to investigate the effects of C28R2 on the oligomeric state of the Ca-ATPase in the SR membrane. The addition of C28R2 at low and high Ca^{2+} results in a decreased amplitude of anisotropy decay in both skeletal (Fig. 4) and cardiac (Fig. 5) SR, with a resulting increase in A_∞ (Fig. 6). In skeletal SR, the large increase in A_∞ at low Ca^{2+} and the moderate increase in A_∞ at high Ca^{2+} with increasing [C28R2] closely correlate with the inhibition of ATPase activity (Fig. 1 *A*). Moreover, the parallel increase in A_∞ values at low and high Ca^{2+} with increasing concentrations of C28R2 correlate well with the parallel decreases in ATPase activity in CSR (Fig. 1 *B*).

A change in the final anisotropy A_∞ may be due to 1) a change in the fraction of immobile Ca-ATPase oligomers or 2) a change in the angle between the membrane normal and the probe's absorption and emission dipoles (Mersol et al., 1995). It has been shown that other perturbants (such as halothane, thapsigargin, lidocaine, and $C_{12}E_8$) affect the rapid submicrosecond motion of the ErITC probe bound to skeletal and cardiac Ca-ATPase by changing the mole fraction of immobile Ca-ATPase oligomers, but do not affect the probe angles (Karon et al., 1995; Mersol et al., 1995; Shi et al., 1996). We fit TPA data to the model of uniaxial rotation (Eqs. 3–5), which explicitly considers both the mole fraction of pumps in immobile oligomers (x_I) and the probe angles. We found that the immobile fraction x_I increased in both skeletal SR and CSR, both at low Ca^{2+} (Fig. 8, *A* and *C*) and at high Ca^{2+} (not shown), but that the the probe angles did not change (Fig. 8, *B* and *D*). Therefore, C28R2-induced increases in A_∞ probably represent Ca-ATPase aggregation, which correlates with enzymatic inhibition.

The erythrocyte plasma membrane Ca-ATPase (PMCA type) is regulated by calmodulin. The enzyme is more active in the dimeric form than in the monomeric form (Kosk-Kosicka et al., 1989). In our studies, C28R2-induced oligomerization (oligomers much larger than dimers) of Ca-ATPase correlates with the inhibition of enzymatic activity. The response of enzymatic activity of skeletal SR to halothane (Karon and Thomas, 1993) at 25°C and the response of CSR to quercetin (Mckenna et al., 1996) were shown to be biphasic. At low concentrations, halothane in skeletal SR (Karon and Thomas, 1993) and quercetin in CSR (Mckenna et al., 1996) activate the Ca-ATPase activity. As the concentration of the drugs increased, Ca-ATPase activity was inhibited. Our previous data suggest that the formation of smaller oligomers in response to low concentration of perturbants correlates with enzyme activation (or no effect), and the formation of larger oligomers in response to higher concentrations correlates with inhibition of the Ca-ATPase in SR. We propose that the inhibition of both skeletal and CSR Ca-ATPase activity in response to C28R2 is due to the formation of much larger oligomers. However, the mechanism of regulation of SERCA1 or SERCA2a by C28R2 cannot be correlated directly with that of PMCA regulation,

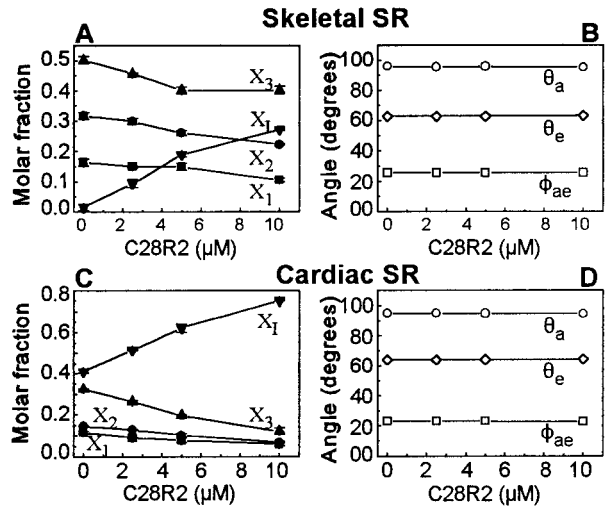

FIGURE 8 Analysis of TPA data based on the model of uniaxial rotation (Eq. 3). The mole fractions (*A, C*) of mobile Ca-ATPase species x_1, x_2, and x_3 and immobile species x_I and the angles describing the orientation of probes relative to the membrane normal (*B, D*) were determined by fitting TPA decays to Eq. 3 ($n = 3$). Results are shown for skeletal SR (*A, B*) and for CSR (*C, D*) at low (0.15 μM) Ca^{2+}.

because the specificity and the site of interaction of this peptide with SERCA isoforms are not understood.

Effects of C28R2 on the conformational state of Ca-ATPase

It has previously been shown in this laboratory that inhibitors that aggregate the Ca-ATPase also shift its conformational equilibrium toward the E2 forms: E2, E2P, and or $E2P_{(2Ca)}$ (Karon et al., 1994). It has also been reported that melittin shifted the enzyme's E1-E2 conformational equilibrium toward E2 at low Ca^{2+} concentration in skeletal SR (Voss et al., 1995). The detergent $C_{12}E_8$ increased the rate of the E2-to-E1 transition and stabilized E2P (Andersen et al., 1983; Champeil et al., 1986; Gould et al., 1986; de Foresta et al., 1989) in skeletal SR. In the present study, in skeletal SR we found that C28R2 shifted the equilibrium toward E2 in the absence of Ca^{2+} (Fig. 7, *top left panel*) and, like $C_{12}E_8$, stabilized the E1 state in the presence of Ca^{2+} (Fig. 7, *top right panel*). Whereas, in CSR, C28R2, like lidocaine, stabilized the E2 conformational state in the absence of Ca^{2+} (Fig. 7, *lower left panel*) and shifted the equilibrium toward the E1 state in the presence of Ca^{2+} (Fig. 7, *lower right panel*). In the presence of PLB Ab, there is a greater increase in fluorescence intensity of FITC-labeled CSR (representing a further stabilization of E2) in response to C28R2 (Fig. 7, *lower left panel*), suggesting that PLB is not responsible for the different effects of C28R2 in CSR compared to skeletal SR. The differences in the effects of C28R2 on SERCA1 at low and high Ca^{2+} may be due to the binding of the peptide to some low-affinity Ca^{2+} binding site, which at high Ca^{2+} is saturated by Ca^{2+} and is no longer available for the binding of C28R2. Alternatively, C28R2 may bind at a site with a specific conformational state in the presence of low Ca^{2+}, and a conformational change at that site in the presence of high Ca^{2+} may prevent the binding of the peptide. The observed differences in conformational equilibrium between skeletal and CSR at low and high Ca^{2+} in response to C28R2 may partly account for the differences in the inhibitory responses to C28R2.

CONCLUSIONS

The effects of C28R2 on the rotational dynamics of the Ca-ATPase show a strong correlation between activity and oligomeric state in skeletal and CSR, indicating that this peptide affects Ca-ATPase activity by causing self-association of the enzyme. C28R2 inhibits and aggregates the Ca-ATPase of both skeletal and CSR. Inhibition and aggregation are Ca-dependent in skeletal SR, but not in CSR. The effects of C28R2 on CSR Ca-ATPase are not significantly altered by PLB Ab. C28R2 stabilizes the E1 conformational state of the Ca-ATPase in skeletal SR, whereas in CSR it stabilizes E2. After the addition of PLB Ab, C28R2 still stabilizes the E2 conformational state in CSR. This suggests that PLB is probably not responsible for the differences observed between skeletal and CSR in response to C28R2.

Despite the significant sequence homology between SERCA1-type (skeletal) and SERCA2-type (cardiac) Ca pumps, there are differences in their response to various inhibitory agents, such as general anesthetics and C28R2. On the other hand, it is remarkable that an autoinhibitory peptide from the PMCA enzyme, which has substantial differences in sequence from the SERCA enzymes, has such potent functional and physical effects on the SERCA pumps. Future studies on the structural bases of these inhibitory effects should shed light on the relationship between structure and function in these Ca-ATPase isoforms.

We thank Dr. Joseph J. Feher, Medical College of Virginia, for the generous gift of CSR. We are also pleased to thank Dr. Larry Jones, Indiana University School of Medicine, for the anti-PLB Ab 2D12. We also thank Brad Karon, Razvan Cornea, Nicoleta Cornea, John Matta, and Robert L. H. Bennett for technical support.

DDT was supported by National Institutes of Health grant GM27906. JTP was supported by National Institutes of Health grant GM28835, and HK by GM50764. LGR was supported by a grant from the American Heart Association.

REFERENCES

Alonso, G. L., and J. P. Hecht. 1990. Thermodynamics of Ca^{2+} transport through sarcoplasmic reticulum membranes during the transient-state of simulated reactions. *J. Theor. Biol.* 147:161–176.

Andersen, J. P., M. L. Maire, K.-H. Ulrich, P. Champeil, and J. V. Moller. 1983. Perturbation of the structure and function of a membranous Ca^{2+}-ATPase by non-solubilizing concentrations of a non-ionic detergent. *Eur. J. Biochem.* 134:205–214.

Belford, G. G., R. L. Belford, and G. Weber. 1972. Dynamics of fluorescence polarization in macromolecules. *Proc. Natl. Acad. Sci. USA.* 69:1392–1393.

Bigelow, D. J., T. C. Squier, and D. D. Thomas. 1986. Temperature dependence of rotational dynamics of protein and lipid in sarcoplasmic reticulum membranes. *Biochemistry.* 25:194–202.

Bigelow, D. J., and D. D. Thomas. 1987. Rotational dynamics of lipid and the Ca-ATPase in sarcoplamic reticulum. The molecular basis of activation by diethyl ether. *J. Biol. Chem.* 262:13449–13456.

Birmachu, W., F. L. Nisswandt, and D. D. Thomas. 1989. Conformational transitions in the calcium adenosine triphosphatase studied by time-resolved fluorescence resonance energy transfer. *Biochemistry.* 28: 3940–3947.

Birmachu, W., and D. D. Thomas. 1990. Rotational dynamics of the Ca-ATPase in sarcoplamic reticulum studied by time-resolved phosphorescence anisotropy. *Biochemistry.* 29:3904–3914.

Cantilina, T., Y. Sagara, G. Inesi, and L. R. Jones. 1993. Comparative studies of cardiac and skeletal sarcoplasmic reticulum ATPases. Effect of a phospholamban antibody on enzyme activation by Ca^{2+}. *J. Biol. Chem.* 268:17018–17025.

Champeil, P., M. L. Maire, J. P. Andersen, F. Guillain, M. Gingold, S. Lund, and J. V. Moller. 1986. Kinetic characterization of the normal and detergent-perturbed reaction cycles of the sarcoplasmic reticulum calcium pump. Rate-limiting step(s) under different conditions. *J. Biol. Chem.* 261:16372–16384.

de Foresta, B., M. le Maire, S. Orlowski, P. Champeil, S. Lund, J. V. Moller, F. Michelangeli, and A. G. Lee. 1989. Membrane solubilization by detergent: use of brominated phospholipids to evaluate the detergent-induced changes in Ca^{2+}-ATPase/lipid interaction. *Biochemistry.* 28: 2558–2567.

Eads, T. M., D. D. Thomas, and R. H. Austin. 1984. Microsecond rotational motions of eosin-labeled myosin measured by time-resolved anisotropy of absorption and phosphorescence. *J. Mol. Biol.* 179:55–81.

Enyedi, A., A. G. Filoteo, G. Gardos, and J. T. Penniston. 1991. Calmodulin-binding domains from isozymes of the plasma membrane Ca^{2+} pump have different regulatory properties. *J. Biol. Chem.* 266: 8952–8956.

Enyedi, A., and J. T. Penniston. 1993. Autoinhibitory domains of various Ca^{2+} transporters cross-react. *J. Biol. Chem.* 268:17120–17125.

Feher, J. J., and F. N. Briggs. 1983. Determinants of calcium loading at steady state in sarcoplasmic reticulum. *Biochim. Biophys. Acta.* 727: 389–402.

Fernandez, J. L., M. Rosemblatt, and C. Hidalgo. 1980. Highly purified sarcoplasmic reticulum vesicles are devoid of Ca^{2+}-independent ("basal") ATPase activity. *Biochim. Biophys. Acta.* 599:552–568.

Froud, R. J., and A. G. Lee. 1986. Conformational transitions in the Ca^{2+} + Mg^{2+}-activated ATPase and the binding of Ca^{2+} ions. *Biochem. J.* 237:197–206.

Gould, G. W., J. M. East, R. J. Froud, J. M. Mowhirter, H. I. Stefanova, and A. G. Lee. 1986. A kinetic model for the Ca^{2+} + Mg^{2+}-activated ATPase of sarcoplasmic reticulum. *Biochem. J.* 237:217–227.

James, P., M. Inui, M. Tada, M. Chiesi, and E. Carafoli. 1989a. Nature and site of phospholamban regulation of the Ca^{2+} pump of sarcoplasmic reticulum. *Nature.* 342:90–92.

Karon, B. S., L. G. Geddis, H. Kutchai, and D. D. Thomas. 1995. Anesthetics alter the physical and functional properties of the Ca-ATPase in cardiac sarcoplasmic reticulum. *Biophys. J.* 68:936–945.

Karon, B. S., J. E. Mahaney, and D. D. Thomas. 1994. Halothane and cyclopiazonic acid modulate Ca-ATPase oligomeric state and function in sarcoplasmic reticulum. *Biochemistry.* 33:13928–13937.

Karon, B. S., and D. D. Thomas. 1993. Molecular mechanism of Ca-ATPase activition by halothane in sarcoplasmic reticulum. *Biochemistry.* 32:7503–7511.

Kosk-Kosicka, D., T. Bzdega, and A. Wawrzynow. 1989. Fluorescence energy transfer studies of purified erythrocyte Ca^{2+}-ATPase. Ca^{2+}-regulated activation by oligomerization. *J. Biol. Chem.* 264: 19495–19499.

Kutchai, H., J. E. Mahaney, L. M. Geddis, and D. D. Thomas. 1994. Hexanol and lidocaine affect the oligomeric state of the Ca-ATPase of sarcoplasmic reticulum. *Biochemistry.* 33:13208–13222.

Lindemann, J. P., L. R. Jones, D. R. Hathaway, and B. G. Henry. 1983. Beta-adrenergic stimulation of phospholamban phosphorylation and Ca^{2+}-ATPase activity in guinea pig ventricles. *J. Biol. Chem.* 258: 464–471.

Ludescher, R. D., and D. D. Thomas. 1988. Microsecond rotational dynamics of phosphorescent-labeled muscle cross-bridges. *Biochemistry.* 27:3343–3351.

Mahaney, J. E., J. Kleinschmidt, D. Marsh, and D. D. Thomas. 1992. Effects of melittin on lipid-protein interactions in sarcoplasmic reticulum membranes. *Biophys. J.* 63:1513–1522.

Mahaney, J. E., and D. D. Thomas. 1991. Effects of melittin on molecular dynamics and Ca-ATPase activity in sarcoplasmic reticulum membranes: electron paramagnetic resonance. *Biochemistry.* 30: 7171–7180.

Mckenna, E., J. S. Smith, K. E. Coll, E. K. Mazack, E. J. Mayer, J. Antanavage, R. T. Wiedmann, and R. G. Johnson, Jr. 1996. Dissociation of phospholamban regulation of cardiac sarcoplasmic reticulum Ca^{2+}-ATPase by quercetin. *J. Biol. Chem.* 271:24517–24525.

Mersol, J. V., H. Kutchai, J. E. Mahaney, and D. D. Thomas. 1995. Self-association accompanies inhibition of Ca-ATPase by thapsigargin. *Biophys. J.* 68:208–215.

Nakamura, J., T. Wang, L.-I. Tsai, and A. Schwartz. 1983. Properties and characterization of a highly purified sarcoplasmic reticulum Ca^{2+}-ATPase from dog cardiac and rebbit skeletal muscle. *J. Biol. Chem.* 258:5079–5083.

Sagara, Y., J. B. Wade, and G. Inesi. 1992. A conformational mechanism for formation of a dead-end complex by the sarcoplasmic reticulum ATPase with thapsigargin. *J. Biol. Chem.* 267:1286–1292.

Sham, J. S. K., L. R. Jones, and M. Morad. 1991. Phospholamban mediates the beta-adrenergic-enhanced Ca^{2+} uptake in mammalian ventricular myocytes. *Am. J. Physiol.* 261:H1344–H1349.

Shi, Y., B. S. Karon, H. Kutchai, and D. D. Thomas. 1996. Phospholamban-dependent effects of $C_{12}E_8$ on calcium transport and molecular dynamics in cardiac sarcoplasmic reticulum. *Biochemistry.* 35: 13393–13399.

Squier, T. C., S. E. Hughes, and D. D. Thomas. 1988a. Rotational dynamics and protein-protein interactions in the Ca-ATPase mechanism. *J. Biol. Chem.* 263:9162–9170.

Squier, T. C., and D. D. Thomas. 1988. Relationship between protein rotational dynamics and phosphoenzyme decomposition in the sarcoplasmic reticulum Ca-ATPase. *J. Biol. Chem.* 263:9171–9177.

Strehler, E. E. 1991. Recent advances in the molecular characterization of plasma membrane Ca^{2+} pumps. *J. Membr. Biol.* 120:1–15.

Szabo, A. 1984. Theory of fluorescence depolarization in macromolecules and membranes. *J. Chem. Phys.* 81:150–166.

Tada, M., and A. M. Katz. 1982. Phosphorylation of the sarcoplasmic reticulum and sarcolemma. *Annu. Rev. Physiol.* 44:401–423.

Verma, A. K., A. G. Filoteo, D. R. Standford, E. D. Wieben, J. T. Penniston, E. E. Strehler, R. Fischer, R. Heim, G. Vogel, S. Matthews, M. Strehler-Page, P. James, T. Vorherr, J. Krebs, and E. Carafoli. 1988. Complete primary structure of a human plasma membrane Ca^{2+} pump. *J. Biol. Chem.* 263:14152–14159.

Vorherr, T., M. Chiesi, R. Schwaller, and E. Carafoli. 1992. Regulation of the calcium ion pump of sarcoplasmic reticulum: reversible inhibition by phospholamban and by the calmodulin binding domain of the plasma membrane calcium ion pump. *Biochemistry.* 31:371–376.

Voss, J., D. Hussey, W. Birmachu, and D. D. Thomas. 1991. Effects of melittin on molecular dynamics and Ca-ATPase activity in sarcoplamic reticulum membranes: time-resolved optical anisotropy. *Biochemistry.* 30:7498–7506.

Voss, J., L. R. Jones, and D. D. Thomas. 1994. The physical mechanism of calcium pump regulation in the heart. *Biophys. J.* 67:190–196.

Voss, J., J. E. Mahaney, L. R. Jones, and D. D. Thomas. 1995. Molecular dynamics in mouse atrial tumor sarcoplasmic reticulum. *Biophys. J.* 68:1787–1795.